Contribution from the Department of Chemistry,
The University of Mississippi, University, Mississippi 38677

Lower Valence Fluorides of Vanadium. 6. Dependence of Structure and Magnetic Properties of the Pseudohexagonal A_xVF_3 Compounds on Composition

Y. S. HONG, R. F. WILLIAMSON, and W. O. J. BOO*

Received April 2, 1980

The pseudohexagonal A_xVF_3 compounds are distorted to two unique orthorhombic unit cells. In the K_xVF_3, Rb_xVF_3, and Tl_xVF_3 systems a transition occurs from the first kind to the second kind at $x \approx 0.26$, 0.24, and 0.24, respectively. The Cs_xVF_3 system is orthorhombic of the second kind over its entire composition range. Four stoichiometric phases were observed within the composition spans of the pseudohexagonal A_xVF_3 systems which have compositions $x = 0.167$, 0.222, 0.250, and 0.333. These phases, designated $\alpha(0.167)$, $\alpha(0.222)$, $\alpha(0.250)$, and $\alpha(0.333)$, each have unique modulated structures and may exist simultaneously as composition domains in the same crystalline sample. The $\alpha(0.167)$ phase has the same dimensions as the orthorhombic sublattice unit cell, but, unlike the sublattice which is primitive, the modulated structure is body centered. The $\alpha(0.222)$ phase has the same a and b dimensions as the sublattice, but $c(\text{super}) = {}^3/_2 c(\text{sub})$. The $\alpha(0.250)$ phase has a primitive unit cell with dimensions $a(\text{super}) = 2a(\text{sub})$, $b(\text{super}) = 3b(\text{sub})$, and $c(\text{super}) = 2c(\text{sub})$. In the $\alpha(0.333)$ phase, A^+ sites are completely filled; hence, its unit cell is not different from that of the parent lattice. All four phases were found in the Rb_xVF_3 and Tl_xVF_3 systems. Only the $\alpha(0.167)$, $\alpha(0.222)$, and $\alpha(0.333)$ phases exist in the K_xVF_3 system, but the Cs^+ ions in the Cs_xVF_3 system appear to be mostly random. Magnetic measurements revealed an induced moment to be associated with the $\alpha(0.222)$ phase.

Introduction

In the third paper of this series,[1] some structural properties of the pseudohexagonal A_xVF_3 systems (where A = K, Rb, Tl, or Cs and x varies from approximately 0.2 to 0.3) were reported on samples from the "A" series. These fluorides are analogues of the hexagonal tungsten bronzes, A_xWO_3 (space group $P6_3/mcm$).[2] Distortions were found in the fluorides which lower their symmetry from hexagonal to orthorhombic in two unique ways. The distinction between the two is dramatized by the ratio of orthohexagonal dimensions $|a|/3^{1/2}|b|$ which is either greater than unity (first kind) or less than unity (second kind). For low values of x, evidence of atomic ordering was also reported. Electron diffraction photographs also indicated orthorhombic symmetry and confirmed that more than one ordered arrangement existed within a single phase.[3] These materials were found to order magnetically above 4.2 K;[4] however, results appeared erratic as some samples displayed antiferromagnetic behavior while others appeared to have small induced moments. Furthermore, measurements on one tiny single crystal revealed its moment to be parallel to the pseudohexagonal c axis.[4]

For establishment of a relationship between structure, physical properties, and composition, a new series of samples which differed by very small increments of composition were prepared and studied. This group of samples, designated as the "B" series, includes the tetragonal tungsten-bronze-like system K_xVF_3, which was reported in a previous paper,[5] the hexagonal tungsten-bronze-like systems reported in this paper, and the modified pyrochlores Rb_xVF_3 and Cs_xVF_3 which will be reported in a following paper.

Experimental Section

The same starting materials and solid-state synthesis techniques were employed for these compounds as previously described for the "A" series.[1] They are designated "B" series in this work and were prepared in 1.91-cm diameter by 3.18-cm length molybdenum containers. Vacuum encapsulation was done by electron-beam welding at the University of Mississippi. Products were analyzed optically by stereoscopic and polarized microscopy. Chemical analyses were performed by Galbraith Laboratories. Vanadium was determined volumetrically (±0.1%), fluorine by specific ion electrode (±0.3% of actual value), and potassium, rubidium cesium, or thallium by atomic absorption (±2%). Nominal values, however, are employed in the text and tables as well as on the plots. Samples were characterized by Guinier-Hägg X-ray techniques using Cu $K\alpha_1$ and Cr $K\alpha_1$ radiations. Magnetic measurements were made from 4.2 to 300 K between 0.14 and 10 kG with a Foner-type PAR vibrating-sample magnetometer equipped with a Janis liquid-helium Dewar, gallium arsenide temperature controller, and copper–constantan thermocouples. Magnetic fields were measured with a F. W. Bell hall-probe gaussmeter, Model 8860. Magnetic data were corrected for core diamagnetism and an additional temperature-independent orbital paramagnetic correction of 6×10^{-4} cm^3 mol^{-1} was made for the V^{3+} ion.

Results

The pseudohexagonal phase is opaque except in very thin sections where its transmitted color is brownish red. Samples at the lower limit of the composition range contained some VF_3 (green). Those at the upper limit contained some $A_{0.5}VF_3$ phase (brownish red), except for $Tl_{0.5}VF_3$ which does not form. Samples $Tl_{0.275}VF_3$, $Tl_{0.300}VF_3$, and $Tl_{0.320}VF_3$ appeared metallic to reflected light but did not appear different from the other samples when examined by transmitted light. Small amounts of unreacted VF_2 (blue) were found in $Rb_{0.250}VF_3$, $Rb_{0.275}VF_3$, $Tl_{0.275}VF_3$, $Cs_{0.275}VF_3$, $Cs_{0.300}VF_3$, and $Cs_{0.320}VF_3$. VF_3 was too finely divided for complete removal from the $A_{0.180}VF_3$ samples, and the tetragonal $K_{0.5}VF_3$ phase could not be effectively removed from $K_{0.300}VF_3$ or $K_{0.275}VF_3$. The pyrochlore-like phases $Rb_{0.5}VF_3$ and $Cs_{0.5}VF_3$, as well as VF_2, were successfully removed from all samples before chemical analyses, X-ray diffraction photographs, and magnetic measurements were made. Chemical analyses are shown in Table I. On the basis of these analyses and the amounts of VF_3 or $A_{0.5}VF_3$ estimated from optical microscope analyses, X-ray diffraction photographs, or magnetic data, the composition limits of the four systems are $K_{0.19}VF_3$–$K_{0.27}VF_3$, $Rb_{0.19}VF_3$–$Rb_{0.32}VF_3$, $Cs_{0.19}VF_3$–$Cs_{0.31}VF_3$, and $Tl_{0.19}VF_3$–$Tl_{0.30}VF_3$. These limits are accurate within ±0.01 and are in agreement with those obtained from the "A" series.

X-ray Diffraction. All of the A_xVF_3 pseudohexagonal samples were fitted to an orthorhombic sublattice unit cell having dimensions $a \approx 13$, $b \approx 7.4$, and $c \approx 7.5$ Å. Table II gives a summary of these dimensions and the distortion ratio $|a|/3^{1/2}|b|$. For a true orthohexagonal unit cell, this ratio is unity.

(1) Y. S. Hong, R. F. Williamson, and W. O. J. Boo, *Inorg. Chem.*, **18**, 2123 (1979).
(2) A. Magnéli, *Acta Chem. Scand.*, **7**, 315 (1953).
(3) R. Langley, D. Rieck, H. Eick, L. Eyring, R. F. Williamson, and W. O. J. Boo, *Mater. Res. Bull.*, **13**, 1297 (1978).
(4) Y. F. Lee, R. F. Williamson, and W. O. J. Boo, *Adv. Chem. Ser.*, in press.
(5) Y. S. Hong, R. F. Williamson, and W. O. J. Boo, *Inorg. Chem.*, *19*, 2229 (1980).

0020-1669/81/1320-0403$01.00/0

Table I. Chemical Analysis of A_xVF_3 Compounds

sample designation	element	% calcd	% found	formula exptl	formula theor
B-K200VF3	K	6.76	6.93	$K_{0.206}VF_{2.70}$	$K_{0.20}VF_3$
	V	44.01	43.93		
	F	49.24	44.17		
B-K225VF3	K	7.54	7.72	$K_{0.231}VF_{3.00}$	$K_{0.225}VF_3$
	V	43.64	43.58		
	F	48.82	48.81		
B-K250VF3	K	8.30	8.48	$K_{0.255}VF_{2.98}$	$K_{0.25}VF_3$
	V	43.28	43.29		
	F	48.42	48.14		
B-RB200VF3	Rb	13.67	13.38	$Rb_{0.197}VF_{3.03}$	$Rb_{0.20}VF_3$
	V	40.74	40.49		
	F	45.59	45.75		
B-RB225VF3	Rb	15.12	14.87	$Rb_{0.222}VF_{3.00}$	$Rb_{0.225}VF_3$
	V	40.06	39.96		
	F	44.82	44.71		
B-RB250VF3	Rb	16.52	16.25	$Rb_{0.246}VF_{2.97}$	$Rb_{0.25}VF_3$
	V	39.40	39.44		
	F	44.08	43.70		
B-RB275VF3	Rb	17.88	17.53	$Rb_{0.271}VF_{2.99}$	$Rb_{0.275}VF_3$
	V	38.76	38.59		
	F	43.36	42.98		
B-RB300VF3	Rb	19.20	18.94	$Rb_{0.297}VF_{3.03}$	$Rb_{0.30}VF_3$
	V	38.14	37.98		
	F	42.67	42.87		
B-RB320VF3	Rb	20.22	19.95	$Rb_{0.318}VF_{3.02}$	$Rb_{0.32}VF_3$
	V	37.66	37.45		
	F	42.13	42.22		
B-CS200VF3	Cs	19.76	19.73	$Cs_{0.201}VF_{3.02}$	$Cs_{0.20}VF_3$
	V	37.87	37.60		
	F	42.37	42.37		
B-CS225VF3	Cs	21.69	21.49	$Cs_{0.224}VF_{2.97}$	$Cs_{0.225}VF_3$
	V	36.96	36.78		
	F	41.35	40.75		
B-CS250VF3	Cs	23.54	21.93	$Cs_{0.226}VF_{2.94}$	$Cs_{0.25}VF_3$
	V	36.09	37.25		
	F	40.38	40.80		
B-CS275VF3	Cs	25.30	25.03	$Cs_{0.273}VF_{3.02}$	$Cs_{0.275}VF_3$
	V	35.26	35.19		
	F	39.45	39.67		
B-CS300VF3	Cs	26.98	26.63	$Cs_{0.299}VF_{2.98}$	$Cs_{0.30}VF_3$
	V	34.46	34.20		
	F	38.56	38.03		
B-CS320VF3	Cs	28.27	27.95	$Cs_{0.316}VF_{3.01}$	$Cs_{0.32}VF_3$
	V	33.86	33.90		
	F	37.88	38.02		
B-TL200VF3	Tl	27.47	27.59	$Tl_{0.202}VF_{3.04}$	$Tl_{0.20}VF_3$
	V	34.23	34.09		
	F	38.30	38.58		
B-TL225VF3	Tl	29.87	29.81	$Tl_{0.226}VF_{3.04}$	$Tl_{0.225}VF_3$
	V	33.10	32.89		
	F	37.03	37.26		
B-TL250VF3	Tl	32.13	32.18	$Tl_{0.242}VF_{2.77}$	$Tl_{0.25}VF_3$
	V	32.03	33.17		
	F	35.84	34.24		
B-TL275VF3	Tl	34.24	34.71	$Tl_{0.268}VF_{2.68}$	$Tl_{0.275}VF_3$
	V	31.04	32.30		
	F	34.72	32.31		
B-TL300VF3	Tl	36.23	36.41	$Tl_{0.301}VF_{2.97}$	$Tl_{0.30}VF_3$
	V	30.10	30.20		
	F	33.68	33.40		
B-TL320VF3	Tl	37.73	37.74	$Tl_{0.320}VF_{2.95}$	$Tl_{0.32}VF_3$
	V	29.39	29.41		
	F	32.88	32.34		

In the K, Rb, and Tl systems, several reflections indexed to the orthorhombic unit cells described above have maximum intensities at the lowest value of x but decrease in intensity as x increases. All of these reflections met the special conditions l = odd and $h + k + l = 2n$. A few of these reflections were also observed in the Cs system (minimum x) but were much weaker in intensity. In the K, Rb, and Tl systems, several reflections which could not be indexed to the sublattice unit cell showed strongest intensities at $x = 0.225$. These reflections were fitted to superlattice unit cells of dimensions a(super) = a(sub), b(super) = b(sub), and c(super) = $^3/_2c$-(sub). All of these reflections obeyed the selection rule $h + k = 2n$. Still another superlattice was found in the Rb and Tl systems which was optimum at $x = 0.25$. This superlattice has dimensions a(super) = $2a$(sub), b(super) = $3b$(sub), and c(super) = $2c$(sub), but no selection rules were found. Table III shows the low-angle Guinier–Hägg data for the Rb system in which Cr $K\alpha_1$ radiation was used. This table is divided into two parts: the orthorhombic structure of the first kind is on the left and the second kind is on the right. The column on the far left gives the hexagonal indicies from which the orthorhombic indicies are derived. These indicies correspond to the hexagonal tungsten bronze unit cell with $a \approx 7.4$ and $c \approx 7.5$ Å. The second column from the left gives orthorhombic indicies of the first kind, and the column on the far right shows orthorhombic indicies of the second kind. Miller indicies of the modulated structures which are optimum in samples $Rb_{0.180}VF_3$, $Rb_{0.225}VF_3$, and $Rb_{0.250}VF_3$ are indicated by single, double, and triple asterisks, respectively. The observed d values and their intensities are given directly above the calculated d values. In some cases, two calculated d's which are close in value were observed as a single reflection, in which case, the observed value appears only once above the two calculated values.

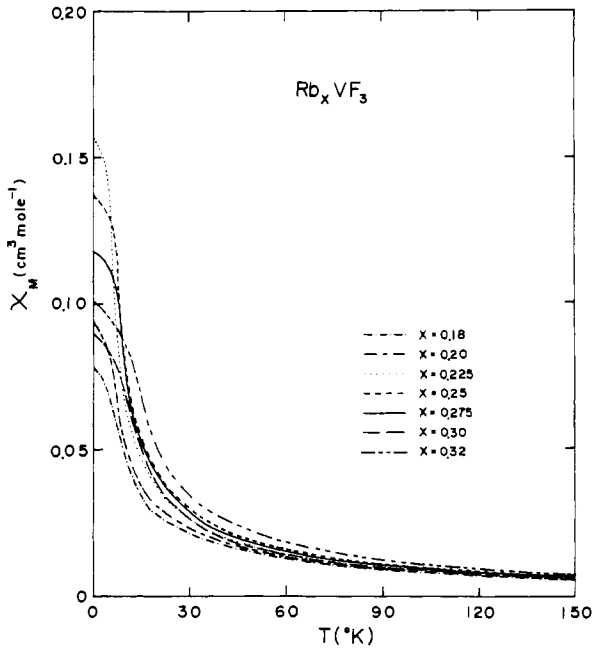

Figure 1. Magnetic susceptibilities of Rb_xVF_3 vs. temperature at 10 kG.

Magnetic Measurements. Magnetic susceptibilities vs. temperature of the Rb_xVF_3 samples are shown in Figure 1. Profiles of these plots are typical of ferrimagnetic materials and are characteristic of all the pseudohexagonal A_xVF_3 compounds. The values of the susceptibilities extrapolated to 0 K suggest the samples have spontaneous magnetic moments of different magnitudes with a maximum moment near $x = 0.225$. These plots, however, do not explicitly define a magnetic ordering temperature.

Inverse susceptibilities vs. temperature of the Rb_xVF_3 samples are shown in Figure 2. The $Rb_{0.320}VF_3$ sample suggests that antiferromagnetic ordering occurs at about 8 K, as a change of slope occurs at that temperature. A change of slope was observed in χ^{-1} vs. T plots of all the Cs_xVF_3 samples near 20 K, but, as in the other Rb_xVF_3 samples, no such feature was found for the K_xVF_3 and Tl_xVF_3 samples. The plot of $Rb_{0.300}VF_3$ does show an anomalous change of slope at about

Table II. Summary of Lattice Constants (A ±0.05%) and Distortion Ratios of Pseudohexagonal (Orthorhombic) A_xVF_3

sample designation	copper data	distortion ratio	chromium data	distortion ratio	sample designation	copper data	distortion ratio	chromium data	distortion ratio
$K_{0.180}VF_3$	12.897	1.007	12.895	1.007	$Cs_{0.200}VF_3$	12.955	0.997	12.964	0.998
	7.395		7.393			7.502		7.497	
	7.531		7.529			7.639		7.638	
$K_{0.200}VF_3$	12.901	1.007	12.896	1.007	$Cs_{0.225}VF_3$	12.961	0.997	12.958	0.997
	7.399		7.397			7.506		7.505	
	7.532		7.531			7.642		7.655	
$K_{0.225}VF_3$	12.888	1.006	12.886	1.006	$Cs_{0.250}VF_3$	12.988	0.998	12.976	0.998
	7.399		7.398			7.513		7.507	
	7.526		7.525			7.663		7.654	
$K_{0.250}VF_3$	12.898	1.006	12.894	1.006	$Cs_{0.275}VF_3$	12.989	0.998	12.979	0.998
	7.402		7.402			7.515		7.509	
	7.531		7.532			7.681		7.667	
$K_{0.275}VF_3$	12.800	0.991	12.792	0.992	$Cs_{0.300}VF_3$	12.991	0.998	12.987	0.998
	7.455		7.449			7.517		7.513	
	7.531		7.529			7.675		7.670	
$Rb_{0.180}VF_3$	12.920	1.005	12.921	1.006	$Cs_{0.320}VF_3$	12.988	0.998	12.980	0.997
	7.422		7.419			7.515		7.517	
	7.560		7.560			7.691		7.685	
$Rb_{0.200}VF_3$	12.921	1.005	12.921	1.005	$Tl_{0.180}VF_3$	12.935	1.005	12.932	1.005
	7.426		7.424			7.432		7.427	
	7.560		7.561			7.565		7.564	
$Rb_{0.225}VF_3$	12.911	1.004	12.913	1.004	$Tl_{0.200}VF_3$	12.939	1.005	12.934	1.005
	7.428		7.428			7.434		7.432	
	7.565		7.561			7.567		7.566	
$Rb_{0.250}VF_3$	12.835	0.991	12.834	0.991	$Tl_{0.225}VF_3$	12.930	1.004	12.932	1.004
	7.476		7.474			7.437		7.436	
	7.569		7.561			7.566		7.568	
$Rb_{0.275}VF_3$	12.837	0.992	12.835	0.992	$Tl_{0.250}VF_3$	12.853	0.992	12.857	0.993
	7.473		7.472			7.481		7.478	
	7.575		7.563			7.569		7.569	
$Rb_{0.300}VF_3$	12.833	0.992	12.832	0.992	$Tl_{0.275}VF_3$	12.851	0.991	12.847	0.991
	7.467		7.469			7.484		7.482	
	7.586		7.578			7.573		7.572	
$Rb_{0.320}VF_3$	12.828	0.992	12.829	0.992	$Tl_{0.300}VF_3$	12.851	0.991	12.849	0.992
	7.468		7.465			7.487		7.478	
	7.586		7.581			7.577		7.581	
$Cs_{0.180}VF_3$	12.953	0.997	12.951	0.997	$Tl_{0.320}VF_3$	12.847	0.990	12.841	0.990
	7.504		7.503			7.489		7.489	
	7.639		7.637			7.583		7.580	

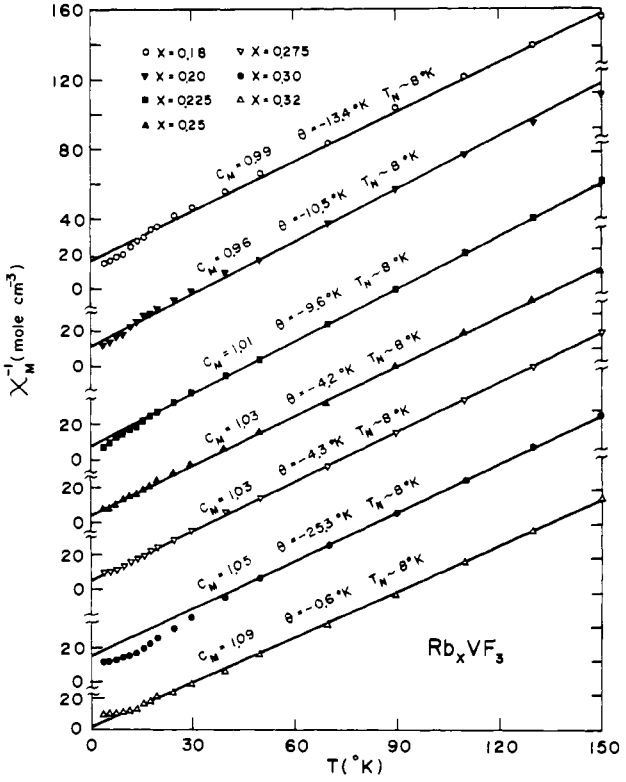

Figure 2. Inverse magnetic susceptibilities of Rb_xVF_3 vs. temperature at 10 kG.

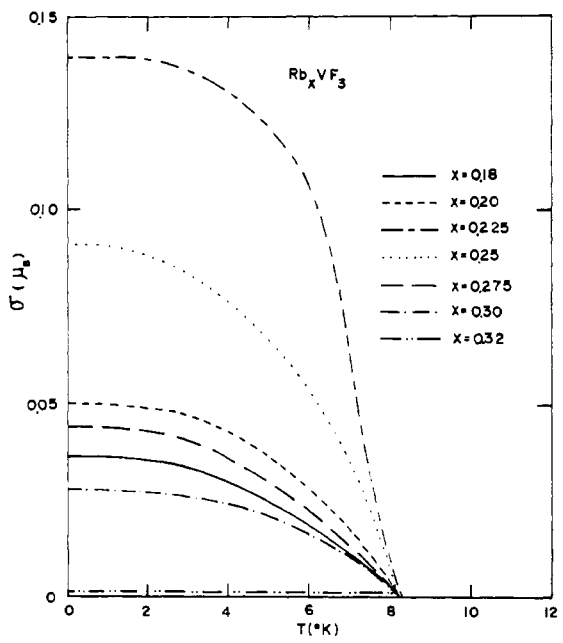

Figure 3. Induced magnetic moments of Rb_xVF_3 vs. temperature for samples cooled in 10-kG field.

30 K which is unexplained at this time.

All the K, Tl, and Rb samples (except $Rb_{0.320}VF_3$) displayed an unusual effect. Linear extrapolations of moments measured at high fields projected moments of significant magnitude at

Table III. Guinier-Hägg X-ray Data for Pseudohexagonal Rb_xVF_3 Cr $K\alpha_1$ Radiation (λ = 2.289 62 A)

hexagonal *hkil*	orthorhombic *hkl*, 1st kind	*d*(obsd)/*I* *d*(calcd)							orthorhombic *hkl*, 2nd kind
		$Rb_{0.180}VF_3$	$Rb_{0.200}VF_3$	$Rb_{0.225}VF_3$	$Rb_{0.250}VF_3$	$Rb_{0.275}VF_3$	$Rb_{0.300}VF_3$	$Rb_{0.320}VF_3$	
					15.152/W^{-1}	15.103/W^{-5}			
					15.122	15.126			001***
		11.359/W^{-3}	11.343/W^{-1}	11.366/W^{-1}	11.355/W^{-3}	11.351/W^{-3}			
	001**	11.340	11.342	11.341	11.342	11.362			001**
					7.587/W^{-2}				
					7.561				002***
		6.546/M^{+}	6.555/M	6.477/W^{-5}					
	101*	6.525	6.526	6.525					
		6.475/M	6.477/M	6.444/W	6.465/W^{-1}	6.465/W^{-1}	6.475/W^{-3}	6.478/W^{-3}	
$10\bar{1}0$	200	6.460	6.461	6.457	6.459	6.458	6.455	6.452	110
	110	6.434	6.437	6.439	6.427	6.418	6.416	6.415	200
					5.948/W^{-1}	5.969/W^{-4}			
					5.940	5.939			231***
					5.919/W^{-2}	5.910/W^{-5}			
					5.907	5.908			401***
		5.681 W^{-4}	5.692 W^{-1}	5.674 W	5.678/W^{-3}	5.632/W^{-4}			
	002**	5.670	5.671	5.671	5.671	5.681			002**
		5.615/W^{-4}	5.621/W^{-1}	5.606/W^{+}	5.608/W^{-2}	5.615/W^{-3}			
	201**	5.613	5.614	5.611	5.612	5.607			111**
	111**	5.596	5.598	5.599	5.585	5.500			201**
		5.308/W^{+}	5.314/W	5.291/W^{-5}					
	011*	5.295	5.297	5.299					
					5.152/W^{-4}				
					5.149				141***
					5.056/W^{-1}				
					5.057				322***
					4.910/W^{-1}				
					4.911				232***
					4.893				402***
		4.265/W^{-1}	4.265/W	4.258/M	4.262/W^{-1}	4.264/W^{-2}	4.266/W^{-5}		
	202**	4.261	4.262	4.261	4.261	4.262	4.266		112**
	112**	4.254	4.255	4.256	4.249	4.250	4.254		202**
		4.102/W^{+}	4.104/W	4.094/W^{-6}					
	211*	4.095	4.096	4.096					
					3.978/W	3.977/W^{-5}			
					3.985	3.985			342***
		3.784/M^{+}	3.786/M^{+}	3.779/M	3.787/M	3.789/M	3.795/W^{+}	3.801/W^{+}	
002	002	3.780	3.781	3.780	3.780	3.782	3.789	3.791	002
		3.746/W^{-2}	3.749/W^{-3}						
	301*	3.742	3.743						
		3.728/W	3.730/W^{-2}	3.724/W^{-2}	3.735/W^{-5}	3.741/W^{-5}	3.734/W^{-5}	3.735/W^{-5}	
$11\bar{2}0$	310	3.725	3.725	3.724	3.737	3.727	3.734	3.733	020
		3.712/W^{-3}	3.716/W^{-3}	3.716/W^{-3}	3.715/W^{-3}	3.717/W^{-4}	3.715/W^{-5}	3.711/W^{-5}	
	020	3.710	3.712	3.714	3.713	3.712	3.712	3.711	310
					3.608/W^{-5}				
					3.628				061***
					3.606				631***
			3.539/W^{-3}	3.537/W^{-2}	3.535/W^{-6}				
	311**		3.539	3.538	3.549				021**
	021**		3.528	3.530	3.529				311**
					3.352/W^{-5}				
					3.350				062***
					3.332/W^{-5}				
					3.333				632***
		3.262/S	3.265/S	3.260/S	3.263/S	3.266/S	3.270/S	3.273/S	
$10\bar{1}1$	202	3.263	3.263	3.260	3.263	3.263	3.268	3.268	112
	112	3.259	3.260	3.260	3.257	3.258	3.263	3.264	202
		3.232/S^{-1}	3.233/S^{-1}	3.229/S	3.230/S^{+}	3.231/S^{+}	3.229/S^{+}	3.231/S^{+}	
$20\bar{2}0$	400	3.230	3.230	3.228	3.229	3.229	3.228	3.226	220
		3.219/S	3.221/S	3.219/S	3.208/M	3.211/M	3.210/S^{-1}	3.211/S^{-1}	
	220	3.217	3.219	3.219	3.208	3.209	3.208	3.207	400
		3.109/W^{-5}	3.112/W^{-2}	3.109/W^{-1}	3.107/W^{-5}				
	312**	3.113	3.114	3.113	3.120				022**
	022**	3.104	3.106	3.107	3.106				312**
					3.004/W^{-3}				
					3.002				063***
					2.991/W^{-2}				
					2.989				633***
					2.972/W^{-5}				
					2.970				462***
					2.954/W^{-5}				
					2.954				802***

Table III (*Continued*)

hexagonal *hkil*	orthorhombic *hkl*, 1st kind	*d*(obsd)/*I* *d*(calcd) $Rb_{0.180}VF_3$	$Rb_{0.200}VF_3$	$Rb_{0.225}VF_3$	$Rb_{0.250}VF_3$	$Rb_{0.275}VF_3$	$Rb_{0.300}VF_3$	$Rb_{0.320}VF_3$	orthorhombic *hkl*, 2nd kind
	402**	2.801/W^{-5} 2.807	2.804/W^{-1} 2.807	2.805/W^{-1} 2.806 2.801 W	2.801/W^{-4} 2.806	2.801/W^{-5} 2.806			222**
	222**	2.798	2.799	2.800	2.793	2.793			402**
	411*	2.759/W^{-1} 2.758	2.760/W^{-2} 2.758						
					2.720/W^{-2} 2.719				463***
					2.707/W^{-3} 2.707				803***
$11\bar{2}1$	312	2.654/M^{-1} 2.653	2.654/M 2.654	2.652/M 2.653	2.658/W 2.658	2.660/W 2.658	2.660/W 2.660	2.658/W^{-1} 2.660	002
	022	2.649/W 2.648	2.650/M^{-1} 2.649	2.649	2.650/M^{-1} 2.649	2.652/M^{-1} 2.649	2.653/M^{-1} 2.652	2.655/M^{-1} 2.652	312

* a(super) = a(sub); b(super) = b(sub); c(super) = c(sub). ** a(super) = a(sub); b(super) = b(sub); c(super) = 1.5c(sub). *** a(super) = 2a(sub); b(super) = 3b(sub); c(super) = 2c(sub).

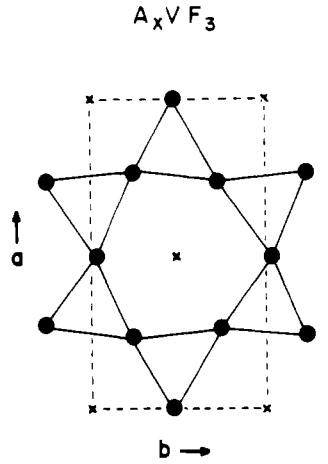

Figure 4. Positions of vanadium ions in the top layer of the orthorhombic A_xVF_3 unit cell.

zero field. Below 5 kG, however, the moment decreases with decreasing field and disappears or becomes slightly negative at zero field. Profiles of the moments of each of the Rb_xVF_3 samples, extrapolated from fields above 5 kG to zero field, vs. temperature are shown in Figure 3. This plot confirms the extrapolated moment has a maximum value near $x = 0.225$, as was suggested by the plots of χ vs. T in Figure 1.

The Cs_xVF_3 samples displayed antiferromagnetic behavior with extrapolated spontaneous moments of a few thousanths of a Bohr magneton, except for $Cs_{0.250}VF_3$ whose moment was 0.01 μ_B. A summary of the magnetic constants C_M, T_N, and Θ, along with the extrapolated magnetic moments of all the pseudohexagonal "B" series samples, are compiled in Table IV. Calculated values of C_M are obtained from

$$C_M = xC_{(2+)} + (1 - x)C_{(3+)}$$

For V^{2+} which is a spin only system

$$C_{(2+)} = \frac{Ng_{(2+)}^2\mu_B^2(\frac{3}{2})(\frac{3}{2} + 1)}{3k}$$

and for V^{3+} in which the orbital moment is largely quenched

$$C_{(3+)} = \frac{Ng_{(3+)}^2\mu_B^2(1)(1 + 1)}{3k}$$

where N is Avogadro's number, $g_{(2+)}$ and $g_{(3+)}$ are the Landé splitting factors for V^{2+} and V^{3+}, respectively, μ_B is the Bohr magneton, and k is the Boltzmann constant.

Table IV. Summary of Magnetic Constants of Pseudohexagonal A_xVF_3 Systems

sample designation	C_M, cm^3 deg mol^{-1} obsd	calcd	Θ, K	T_N, K	σ, μ_B
$K_{0.180}VF_3$	0.95	0.95	−13	8	0.02
$K_{0.200}VF_3$	0.96	0.97	−11	8	0.06
$K_{0.225}VF_3$	0.98	1.00	−6	8	0.19
$K_{0.250}VF_3$	1.00	1.02	−6	8	0.14
$K_{0.275}VF_3$	1.06	1.05	−4	8	0.10
$Rb_{0.180}VF_3$	0.99	0.95	−13	8	0.04
$Rb_{0.200}VF_3$	0.96	0.97	−11	8	0.05
$Rb_{0.225}VF_3$	1.01	1.00	−10	8	0.14
$Rb_{0.250}VF_3$	1.03	1.02	−4	8	0.09
$Rb_{0.275}VF_3$	1.03	1.05	−4	8	0.05
$Rb_{0.300}VF_3$	1.05	1.08	−25	8	0.03
$Rb_{0.320}VF_3$	1.09	1.10	−1	8	0.00
$Tl_{0.180}VF_3$	0.93	0.95	−15	8	0.03
$Tl_{0.200}VF_3$	0.96	0.97	−14	8	0.04
$Tl_{0.225}VF_3$	0.99	1.00	−8	8	0.08
$Tl_{0.250}VF_3$	1.06	1.02	−8	8	0.05
$Tl_{0.275}VF_3$	1.06	1.05	−3	8	0.03
$Tl_{0.300}VF_3$	1.09	1.08	−1	8	0.03
$Tl_{0.320}VF_3$	1.11	1.10	−2	8	0.01
$Cs_{0.180}VF_3$	0.95	0.95	−24	20	
$Cs_{0.200}VF_3$	0.99	0.97	−24	20	
$Cs_{0.225}VF_3$	1.00	1.00	−24	19	
$Cs_{0.250}VF_3$	1.03	1.02	−21	18	0.01
$Cs_{0.275}VF_3$	1.07	1.05	−23	20	
$Cs_{0.300}VF_3$	1.03	1.08	−23	20	
$Cs_{0.320}VF_3$	1.08	1.10	−17	20	

The value of $g_{(2+)}$ was found to be 1.97 in the paramagnetic regions of VF_2[6] and KVF_3,[7] and the average value of $g_{(3+)}$ from the paramagnetic region of VF_3[8] was calculated to be 1.74. From these g values, $C_{(2+)} = 1.820$ and $C_{(3+)} = 0.757$. Calculated values of C_M shown in Table IV are for "nominal" values of x.

Discussion

Figure 4 shows the positions of the vanadium ions in the top layer of the tungsten-bronze-like structure. The second layer of vanadium ions can be visualized by rotating the unit cell 180° about its center. The orthorhombic unit cell is distorted from orthohexagonal by elongating a and shortening b (distortion of the first kind) or vice versa (distortion of the second kind). In the K_xVF_3 system, shown in Table II, a transition from the first kind to the second kind occurs at a

(6) J. W. Stout and H. Y. Lau, *J. Appl. Phys.*, **38**, 1472 (1967).
(7) R. F. Williamson and W. O. J. Boo, *Inorg. Chem.*, **16**, 646 (1977).
(8) A. C. Gossard, H. J. Guggenheim, F. S. L. Hsu, and R. C. Sherwood, *AIP Conf. Proc.*, **No. 5**, 302 (1971).

concentration of $x \approx 0.26$ (between $x = 0.250$ and 0.275), the Rb_xVF_3 and Tl_xVF_3 systems change at $x \approx 0.24$ (between $x = 0.225$ and 0.250), and the Cs_xVF_3 system is distorted to the second kind over its entire composition range. The fact that the distortion is very small, especially in the Cs_xVF_3 system, suggests that the distortion is not simply a collapse of the parent lattice. One possible explanation is that the distortion is a cooperative Jahn–Teller effect. In the hexagonal tungsten-bronze-like structure the vanadium ions are octahedrally coordinated by six fluoride ions. The V^{2+} ion, with electronic configuration $(t_{2g})^3$, has a nondegenerate ground state $^4A_{2g}$, but the V^{3+} ion, with configuration $(t_{2g})^2$, has a degenerate ground state $^3T_{1g}$. According to the Jahn–Teller theorem, orbitally degenerate ground states are not possible in nonlinear systems.[9] Furthermore, there will always be a mechanism for reducing the symmetry of a molecule or a complex such that its ground state will be nondegenerate. Large level splittings are expected in an octahedral environment if the ground state is σ antibonding or σ bonding such as in Cu^{2+} and Cr^{2+}, respectively. Much smaller splittings would be expected if the ground state were π bonding or π antibonding as in (Ti^{2+}, Ti^{3+}, V^{3+}) or (Fe^{2+}, Co^{2+}, Co^{3+}) in octahedral environments, respectively. The Jahn–Teller effect has been predicted for octahedrally coordinated V^{3+}.[10] The reversal in direction of the distortion at a critical composition implies that orientation of the V^{3+} ions in this structure depends on composition or the size of the A^+ ion.

In the X-ray data, certain reflections indexed to the orthorhombic sublattice unit cell were observed to obey the selection rule l = odd, $h + k + l = 2n$. These reflections were quite strong for the minimum values of x in the K, Rb, and Tl systems, and a few, although weaker in intensity, were present in the Cs system. The intensities of these reflections in the former three systems are consistent with atomic ordering of the A^+ ions in partially filled sites. The selection rule indicates the modulated structure is body centered, which would be optimum for half-filled sites ($x = 0.167$). The second modulated structure has a superlattice with the same a and b dimensions as the parent lattice, but its c dimension is $^3/_2$ that of the sublattice. This superlattice was present in the K, Rb, and Tl systems and was optimum at $x = 0.225$. The selection rules indicate this superstructure to be base centered. It is significant that this structure is three layers deep. These conditions are consistent with layers of A^+ ions in the ab plane being completely empty or filled. For the composition $x = 0.222$, two-thirds of the A^+ sites would be filled. Therefore, the layer structure would be a repeat of one empty layer, two filled layers, one empty layer, etc. In the Rb and Tl systems, a third modulated structure was observed to be optimum at the composition $x = 0.25$. This superstructure is much larger than the others, and it is significant that it is four layers deep along the c direction, which is consistent with three-fourths of the A^+ sites being filled ($x = 0.25$). The fact that a and b have dimensions greater than the sublattice unit cell rules out the possibility of the layers of A^+ ions being either completely empty or completely filled, as in the previous superstructure. From Table III, it is seen that reflections from more than one superlattice are present in a single sample. Because the intensities of these superlattice lines are relatively strong, plus the fact they are observed from a powdered sample, suggests the existence of ordered domains of fixed composition, and several of these so-called composition domains can coexist in the same single crystal. It is appropriate to label these domains $\alpha(0.167)$, $\alpha(0.222)$, and $\alpha(0.250)$ in which A^+ sites are $^1/_2$, $^2/_3$, and $^3/_4$ filled, respectively. To be consistent, a fourth domain of completely filled A^+ sites should be called $\alpha(0.333)$. The samples $Rb_{0.180}VF_3$, $Rb_{0.200}VF_3$, and $Rb_{0.225}VF_3$ have variable amounts of $\alpha(0.167)$ and $\alpha(0.222)$. Samples $Rb_{0.250}VF_3$ and $Rb_{0.275}VF_3$ contain observable amounts of $\alpha(0.222)$ and $\alpha(0.250)$ with the remainder being $\alpha(0.333)$, although this latter phase is not verified experimentally because it has no characteristic superlattice.

Inverse magnetic susceptibility vs. temperature plots of sample $Rb_{0.320}VF_3$ and all of the Cs_xVF_3 samples indicate long-range antiferromagnetic ordering sets in at ~8 K and ~20 K, respectively. The inverse susceptibility vs. temperature plots of all the other samples give little or no indication of magnetic ordering. From Figure 3, the existence of induced magnetic moments is an indication of long-range magnetic ordering. In the K, Rb, and Tl systems, T_N is approximately 8 K independent of x. The remarkable feature, however, is that magnitudes of these induced moments depend on x. This feature is dramatized by Figure 5, which is a plot of the

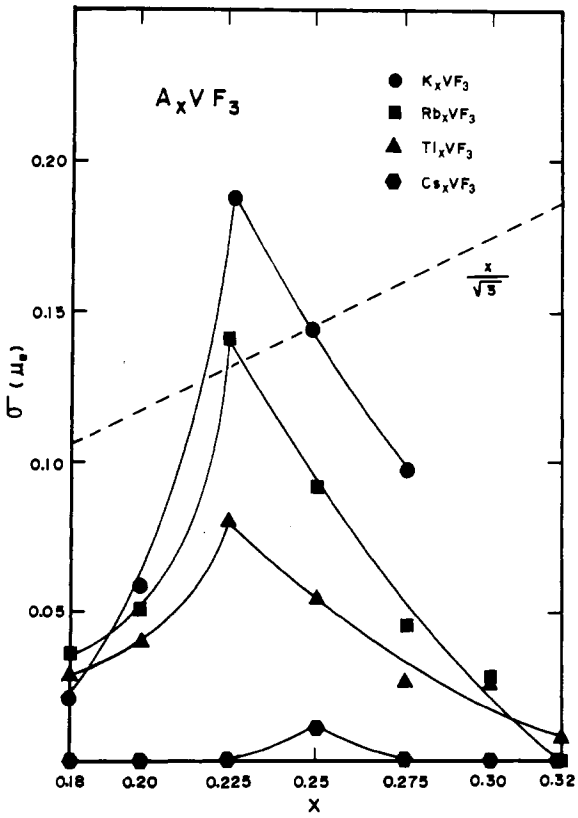

Figure 5. Induced magnetic moments of A_xVF_3 vs. x for samples cooled in 10-kG fields.

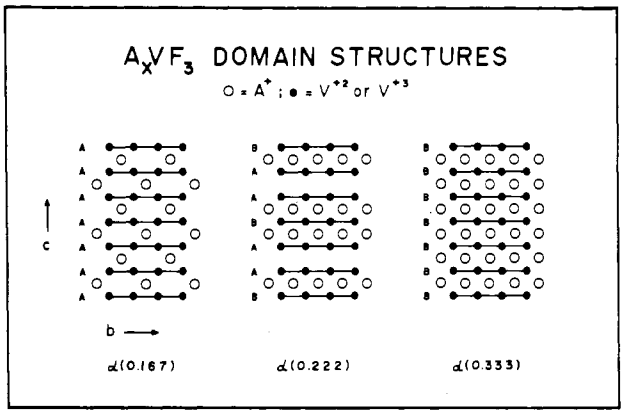

Figure 6. Arrangements of A^+ ions between layers of vanadium ions in $\alpha(0.167)$, $\alpha(0.222)$, and $\alpha(0.333)$ domains.

(9) H. A. Jahn and E. Teller, *Proc. R. Soc. London, Ser. A*, **161**, 220 (1937).
(10) D. Reinen, *J. Solid State Chem.*, **27**, 71 (1979).

induced moments vs. x for each of the four systems. From this plot, one sees immediately that the maximum moment in the K, Rb, and Tl systems occurs at $x = 0.225$. This associates the moment with the $\alpha(0.222)$ phase, which is optimum at that composition and decreases in mole fraction as x increases and decreases from 0.225. In the K system, the magnitude of the moment is greater than in the Rb or Tl systems, but the K system also differs from the Rb and Tl systems in that the $\alpha(0.250)$ phase was not observed. Hence, the mole fraction of $\alpha(0.222)$ is greatest in the K system.

The Cs system appears to have well-behaved magnetic properties. Its magnetic constants Θ and T_N are nearly independent of composition, and their ratio Θ/T_N is approximately unity, as is characteristic of simple antiferromagnetic materials. In the K, Rb, and Tl systems, however, this ratio changes drastically with composition. The value $T_N \approx 8$ is the same for all three systems and is independent of x, but Θ approaches 0 K as x approaches 0.333. This indicates that a ferromagnetic interaction becomes significant as x increases. The fact that Θ changes with x in the K, Rb, and Tl systems, but is virtually independent of x in the Cs system, is a clear indication the superexchange interaction is very sensitive to interatomic distances. In Table IV, C_M(calcd) is in reasonable agreement with C_M(obsd); therefore, one concludes that in the paramagnetic region the orbital moment of V^{3+} is largely quenched in all the pseudohexagonal A_xVF_3 compounds.

From Figure 4, it is clear that nearest-neighboring vanadium ions cannot all be arranged antiparallel, as each pair of nearest neighbors has a common nearest neighbor. There are four of these triangular constraints in the layer of the unit cell shown, or 0.667 constraints per vanadium ion. It is almost certain that the induced magnetic moment of the $\alpha(0.222)$ domain is not the product of a simple two sublattice ferrimagnet. The fact that the magnetic moment is not spontaneous could be a consequence of magnetic domains; however, it is more likely that in a magnetic field the spins within the unit cell are rearranged such that more than half of them are aligned parallel with the field and less than half antiparallel to it. It was demonstrated previously by measurements made on a single crystal of composition $K_{0.20}VF_3$ that ordered spins lie parallel to the pseudohexagonal c axis.[4] If we examine the concept of an ideal ferrimagnet defined specifically for the $A_xV^{II}_xV^{III}_{1-x}F_3$ compounds,[5] we see the remanent moment per vanadium atom would have the value

$$\sigma_{(\|)} = x[g_{(2+)}S_{(2+)} - g_{(3+)}S_{(3+)}]$$

Since one would expect the orbital moment to be totally quenched in the magnetically ordered state, the best approximations for both $g_{(2+)}$ and $g_{(3+)}$ would be 2.0, and

$$\sigma_{(\|)} = x$$

or for a powdered sample

$$\bar{\sigma} = x/3^{1/2}$$

This relationship is shown as a dashed line in Figure 5. The observed moment of sample $K_{0.225}VF_3$ should be less than $x/3^{1/2}$ because this sample contains $\alpha(0.167)$, and probably $\alpha(0.333)$, in addition to $\alpha(0.222)$. It is immediately obvious from Figure 5 that its moment is much too large. We conclude, therefore, that magnetic behavior of $\alpha(0.222)$ cannot be explained by a simple two sublattice model.

The structures of the pseudohexagonal A_xVF_3 phases are very complex. Distortion from hexagonal symmetry is explained as a cooperative Jahn–Teller effect which involves two orientations of the V^{3+} ion. The $\alpha(0.167)$, $\alpha(0.222)$, and $\alpha(0.250)$ phases are a consequence of A^+ ordering which may also be accompanied by V^{2+}–V^{3+} ordering. The $\alpha(0.222)$ phase displays a magnetic moment in a field of 5 kG or greater. This moment is definitely associated with some V^{2+}–V^{3+} ordering pattern in the $\alpha(0.222)$ unit cell. Ordering in the K, Rb, and Tl systems is believed to be basically antiferromagnetic as in the Cs system, the difference being that V^{2+}–V^{3+} as well as Cs^+ is random in the latter. Further investigations into the nature of these phenomena are in progress.

Acknowledgment. The authors gratefully acknowledge the National Science Foundation (Grants DMR 79-00313, DMR 76-83360, DMR 74-11970) for financial support, including the purchase of major equipment, and the University of Mississippi for cost sharing. They also thank NASA Langley Research Center for the loan of an electromagnet and power supply. Appreciation is expressed to the University of Mississippi Computer Center for providing data reduction time.

Registry No. Potassium vanadium fluoride, 55957-20-5; rubidium vanadium fluoride, 63774-72-1; thallium vanadium fluoride, 66792-15-2; cesium vanadium fluoride, 63774-59-4.